4118–4127 *Nucleic Acids Research, 2008, Vol. 36, No. 12* *Published online 10 June 2008*
doi:10.1093/nar/gkn376

Sliding and jumping of single EcoRV restriction enzymes on non-cognate DNA

Isabelle Bonnet[1], Andreas Biebricher[1], Pierre-Louis Porté[1], Claude Loverdo[2], Olivier Bénichou[2], Raphaël Voituriez[2], Christophe Escudé[3], Wolfgang Wende[4], Alfred Pingoud[4] and Pierre Desbiolles[1,*]

[1]Laboratoire Kastler Brossel, ENS, UPMC-Paris 6, CNRS UMR 8552, 24 rue Lhomond, [2]Laboratoire de Physique Théorique de la Matière Condensée, CNRS UMR 7600, Université Pierre et Marie Curie-Paris 6, 4 place Jussieu, [3]Muséum National d'Histoire Naturelle, INSERM U565, CNRS UMR 8646, 43 rue Cuvier, F-75005 Paris, France and [4]Justus-Liebig-Universität Gießen, Institut für Biochemie, FB 8, Heinrich-Buff-Ring 58, D-32392 Gießen, Germany

Received February 26, 2008; Revised May 27, 2008; Accepted May 28, 2008

ABSTRACT

The restriction endonuclease EcoRV can rapidly locate a short recognition site within long non-cognate DNA using 'facilitated diffusion'. This process has long been attributed to a sliding mechanism, in which the enzyme first binds to the DNA via nonspecific interaction and then moves along the DNA by 1D diffusion. Recent studies, however, provided evidence that 3D translocations (hopping/jumping) also help EcoRV to locate its target site. Here we report the first direct observation of sliding and jumping of individual EcoRV molecules along nonspecific DNA. Using fluorescence microscopy, we could distinguish between a slow 1D diffusion of the enzyme and a fast translocation mechanism that was demonstrated to stem from 3D jumps. Salt effects on both sliding and jumping were investigated, and we developed numerical simulations to account for both the jump frequency and the jump length distribution. We deduced from our study the 1D diffusion coefficient of EcoRV, and we estimated the number of jumps occurring during an interaction event with nonspecific DNA. Our results substantiate that sliding alternates with hopping/jumping during the facilitated diffusion of EcoRV and, furthermore, set up a framework for the investigation of target site location by other DNA-binding proteins.

INTRODUCTION

Accelerated target location by site-specific DNA-binding proteins has motivated numerous experimental and theoretical studies for over thirty years (1–7). It is now widely accepted that, in order to reach their target site, proteins first translocate along nonspecific DNA, i.e. move along DNA that does not contain any specific site. The mechanism underlying this so-called 'facilitated diffusion', however, is still under debate. Sliding, a process that involves a linear diffusion along nonspecific DNA, has long been considered as the main mechanism of facilitated diffusion (8). Apart from allowing proteins to carefully scan the DNA, one-dimensional diffusion, by reducing the dimensionality of the space to be explored, can speed up target site location compared with 3D search in solution (9,10). Supporting the linear diffusion hypothesis, recent single-molecule experiments, performed both *in vitro* (11–16) and *in vivo* (17), have shown that various proteins can slide along DNA. Alternatively, fast target location can be ascribed to hopping/jumping (2,18). Hopping and jumping stem from the same mechanism, which involves dissociation, 3D diffusion and re-association of the protein to the same DNA molecule. The distinction between the two processes is based on the location of the re-association site, which is either close to the dissociation location (hopping), or far from it (jumping) (2,18). It was realized early that re-associations of a protein after dissociation from the DNA are highly probable (2), and, recently, this hypothesis was supported by bulk experiments demonstrating a significant contribution of 3D

*To whom correspondence should be addressed. Tel: +33 144 323 380; Fax: +33 144 323 434; Email: pierre.desbiolles@lkb.ens.fr
Correspondence may also be addressed to Andreas Biebricher. Tel: +33 144 323 455; Fax: +33 144 323 434; Email: biebrich@lkb.ens.fr

The authors wish it to be known that, in their opinion, the first two authors should be regarded as joint First Authors

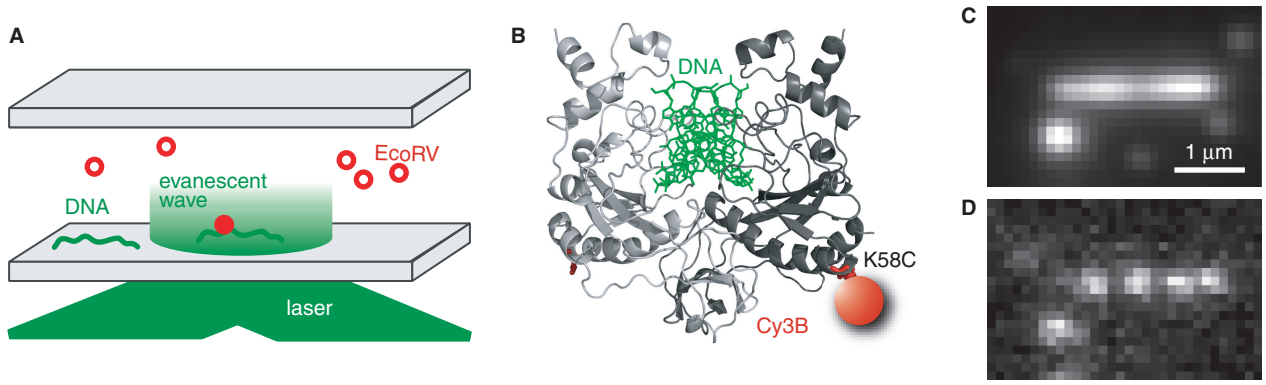

Figure 1. Single-molecule set-up for the study of the facilitated diffusion of EcoRV along nonspecific DNA. (**A**) Biotinylated DNA molecules are attached at both ends to a streptavidin-coated surface. The molecules are in an elongated conformation, but free to fluctuate. Proteins are visualized using Total Internal Reflection Fluorescence Microscopy. (**B**) EcoRV tertiary structure displaying the Cy3B-labelling performed at position 58, remote from the DNA-binding site. (**C**) The accumulation of the fluorescence signal of hundreds of enzymes is used to visualize the elongated DNA (movie of duration ≈150 s, pixel size 126 nm, exposure time 20 ms). Note that, for better visualization, the video sequence was recorded at much higher enzyme concentration than used during single-molecule experiments. Due to the passivation of the surface, only a few proteins stuck to the surface, even at high concentration of enzymes. (**D**) A single frame from the movie depicts four enzymes bound to the DNA. The bright spot in the lower left corner stems from enzyme interactions with a DNA bound by only one end to the surface.

translocations to target site location (18). Besides, jumping allows a protein to rapidly reach DNA sites which are far from the initial binding site, and thus can be considered as complementary to sliding, an inefficient mode of searching over long distances (19). Hopping/jumping may also be more appropriate for an *in vivo* search, as the large number of proteins bound to the DNA makes a sliding motion over large distances almost impossible (20). The most effective target search might actually consist of a balanced combination of both sliding and hopping/jumping, as suggested by recent theoretical studies (21–26). However, in contrast to sliding, 3D translocations have so far not been observed in single-molecule experiments.

Among site-specific DNA-binding proteins, type II restriction enzymes are well-suited for the investigation of facilitated diffusion by *in vitro* kinetic studies (27,28). Specifically, EcoRV has been the subject of intensive research. Translocation of the enzyme from nonspecific DNA to its recognition site was initially attributed to sliding (29). This hypothesis was corroborated by experiments demonstrating that target location is accelerated if the length of nonspecific DNA flanking the EcoRV recognition site is increased (30) and by the study of target search by EcoRV *in vivo* (31). Sliding is also supported by the crystal structure of EcoRV in complex with nonspecific DNA (32), in which the enzyme has an open conformation that sustains the possibility of a linear diffusion along the DNA (33). In addition, facilitated diffusion of EcoRV has been addressed in experiments involving DNA with two recognition sites in close proximity, the interpretation of which suggested that hopping/jumping plays a major role in the process (34). However, alternative interpretation of the experimental data has been proposed which emphasized the role of sliding (35). These conflicting conclusions probably stem from the use of different models that involve successive stages to describe EcoRV-DNA interactions (interaction with nonspecific DNA, association to the target, cleavage of the DNA and subsequent release from the substrate), the features of which are not known in all details. Besides, experimental evidence for hopping/jumping of EcoRV has been provided by recent experiments involving a DNA catenane substrate (36).

A single-molecule approach is an appealing strategy for tackling the question of how EcoRV finds its target site. Recently, the interaction of endonucleases with the DNA has been studied using manipulations of individual DNA molecules with tweezers (37–39). These experiments, however, relied on measurements of forces and DNA length changes, and therefore are not adapted to investigations regarding facilitated diffusion. In contrast, fluorescence microscopy makes it possible to track a labelled enzyme and to observe its translocation path on a DNA molecule. Moreover, the study of facilitated diffusion by single-molecule fluorescence microscopy is not biased by enzyme cleavage kinetics, whereas biochemical experiments usually require DNA cleavage.

We report in this article the direct observation of single fluorescently labelled EcoRV interacting with elongated DNA molecules by Total Internal Reflection Fluorescence Microscopy (TIRFM, see Figure 1A). In order to investigate solely the facilitated diffusion of the enzyme, we used DNA that does not contain any EcoRV cleavage site. Recording the protein trajectories allowed us to establish the sliding of EcoRV along DNA and to determine the linear diffusion coefficient of the enzyme. Concurrently, we observed large translocations of the proteins along the DNA which were orders of magnitude faster than expected for sliding. Experiments performed under flow strongly suggest that these large jumps are due to free 3D excursions. Furthermore, we performed numerical simulations based on a 3D-diffusion model which accounted for both the frequency and the length distribution of the large jumps. We also performed experiments at different salt concentrations, the results of which indicate that not only large jumps, but also smaller jumps that cannot be detected by optical means, may alternate with sliding phases during DNA–EcoRV interaction.

MATERIALS AND METHODS

Enzyme preparation and labelling

Wild type EcoRV is a homodimeric protein that contains one cysteine residue per subunit located close to the core of the protein. We prepared an EcoRV C21S/K58C variant in which the native cysteine residue (C21) was substituted by a serine residue and a single cysteine was inserted at position 58 (33), far from the active center (Figure 1B). Labelling was achieved using a Cy3B-maleimide Mono-Reactive pack (Amersham Bioscience). Unreacted Cy3B-maleimide was removed using a Zeba Micro desalt Spin column (Pierce). The labelling efficiency was about 0.4, estimated using $\varepsilon_{559}{}^{Cy3B} = 1.3 \times 10^5\,M^{-1}\,cm^{-1}$, $\varepsilon_{280}{}^{Cy3B} = 1.5 \times 10^4\,M^{-1}\,cm^{-1}$ and $\varepsilon_{280}{}^{EcoRV} = 4.84 \times 10^4\,M^{-1}\,cm^{-1}$. The EcoRV variant as well as the fluorescent-labelled protein displayed negligible loss of cleavage activity compared to the wildtype enzyme (data not shown). Observation of labelled enzymes stuck to the surface revealed that photobleaching occurred in a maximal number of two steps, which is consistent with the presence of one or two dyes on the protein complex. Single-molecule measurements were performed at pH 7.5 in 20 mM buffer, 10 mM $MgCl_2$, 10–60 mM NaCl, 1 mM DTT and 0.02% v/v blocking reagent (Roche Diagnostics). Experiments were carried out in four different buffers: HEPES (4-(2-Hydroxyethyl) piperazine-1-ethanesulfonic acid), PIPES (1,4-Piperazine-diethanesulfonic acid), PB (sodium phosphate) or Tris (Tris(hydroxymethyl)aminomethane acetate salt), all purchased from Sigma-Aldrich.

DNA preparation and stretching

T7 bacteriophage DNA (Biocentric), which does not contain any recognition site for EcoRV, was cleaved with BsmBI (New England Biolabs). The longest fragment (~8.2 kbp) was ligated to two 500 bp PCR fragments, each containing about 70 biotin-modified uracil bases (Roche Diagnostics), according to a previously published method (40). Glass coverslips were silanized with 0.1% v/v aminopropyl-triethoxysilane (Sigma Chemical) in acidic ethanol. A flow cell was made by adhering, via a parafilm spacer, a silane-coated coverslip to a microscope slide into which two holes had been drilled as inlet and outlet. Biotinylated Blocking Reagent (1 mg/ml, prepared by reaction of 2 µl of Sulfo-NHS-LC-LC-Biotin (Pierce) at 100 mg/ml in DMSO with 200 µl of 2 mg/ml Blocking Reagent (Roche Diagnostics) in PIPES 20 mM, NaCl 100 m, pH 6.8), then streptavidin (0.1 mg/ml in PIPES 20 mM, pH 6.8), were incubated in the cell for 10 min. Subsequent incubation of the biotinylated DNA for a few seconds resulted in the attachment of DNA molecules to the surface by one end. Application of a fast flow (~70 µm/s near the surface) induced the elongation of the DNA and the binding of the second biotinylated DNA end to the surface. The elongated molecules were then stained with a DNA groove-binding dye (SybrGold, Invitrogen) and observed by fluorescence microscopy. We found that the DNA molecules were elongated to about 70% of the contour length. Observation of transverse DNA fluctuations ensured that surface attachment occurred solely via the biotinylated ends (41), while the main part of the DNA was freely accessible in solution. Elongated DNA molecules were stable for hours, and we never observed a detachment of the ends from the surface. In order to reduce nonspecific interactions between the proteins and the surface, residual streptavidin was passivated with biotinylated Blocking Reagent (0.1 mg/ml in 20 mM PIPES, pH 6.8, 50 mM NaCl) for 10 min.

Optical set-up

The flow cell was placed on an inverted microscope (Olympus IX70) equipped with a 60X oil-immersion objective (NA = 1.45, Olympus). After staining, the elongated DNA molecule were located with the aid of a mercury lamp using appropriate excitation and emission filters (480DF40 and longpass 505 LP, respectively, Omega Optical). After recording the positions of the elongated DNA molecules, the dye was removed for further measurements by flushing the flow cell with 2 ml of buffer containing 50 mM $MgCl_2$. We used TIRFM to detect the labelled enzymes, using for excitation a laser at 532 nm with a light intensity of 100 W/cm^2. Fluorescent light was collected via a dichroic mirror (560DRLP, Omega Optical) in combination with a longpass filter (565ALP, Omega Optical) and imaged on an EMCCD Camera (Ixon, Andor Technology) with a 20 ms exposure time. We used a home-made program written in MatLab to fit the point-spread function of the fluorescent spots with a two-dimensional Gaussian function, and to derive the Mean Square Displacement (MSD) from the enzyme trajectories.

RESULTS

Single-molecule assay

We attached biotinylated DNA molecules in an elongated conformation to a streptavidin-coated surface (Figure 1A) using a technique similar to those described in previous publications (41,42). We used a modified T7 DNA fragment (9.2 kbp) which was elongated to 70% of its contour length. EcoRV was labelled with Cy3B at a specific cysteine residue remote from the active center of the protein (Figure 1B). After injection of the fluorescently labeled enzymes in the flow cell, the flow was stopped. At a concentration of EcoRV in the nM range, we detected several enzymes simultaneously interacting with the DNA template, while rarely nonspecific interactions with the surface were observed (Figure 1C and D, and Supplementary Data 3). However, for single-molecule analysis, we reduced the enzyme concentration to 5–20 pM in order to observe, on average, less than one enzyme on the DNA at a given time (Supplementary Data 4 and 5). The position of the enzyme could be determined in each frame, thereby allowing us to reconstruct the enzyme trajectory. The localization accuracy, which was limited by the number of photons accumulated during the exposure time (20 ms), was about 30 nm (Supplementary Data). We checked that the fluorescence signal was due to a single enzyme and that the dye used for labelling did not influence the enzyme dynamics (Supplementary Data).

At low NaCl concentration (10 mM), single enzymes interacted with the DNA on a time-scale of seconds, yielding long enzyme trajectories (typically more than 50 frames). An interaction event ended when we could not detect the enzyme for more than two consecutive frames, either because the enzyme dissociated from the DNA or because of the photobleaching of the dye. We considered for further analysis only interaction events longer than 30 frames (600 ms). The mean time between two consecutive interaction events was about 5–10 s. Since ensemble measurements had indicated an effect of the buffer on the cleavage kinetics (43), experiments were performed at pH 7.5 with four different buffers: HEPES, PIPES, sodium phosphate (PB) and Tris. For each buffer we recorded hundreds of DNA–EcoRV interaction events.

Sliding of EcoRV

A typical single enzyme trajectory is shown in Figure 2A, which displays both the longitudinal (i.e. along the DNA) and transverse (i.e. perpendicular to the DNA and within the focal plane) positions of the enzyme as a function of time. Two processes contribute to the variations of the longitudinal position of the enzymes: the motion along the DNA and the thermal fluctuations of the elongated DNA template (Figure 2A). For each interaction event, we computed the MSD versus time of the enzyme to discriminate between sliding and DNA fluctuations (see Supplementary Data for the calculation of the MSD). The longitudinal and the transverse MSD calculated from a single enzyme trajectory are displayed in Figure 2B. While the transverse MSD is constant, the longitudinal MSD depends linearly on time, as expected for an enzyme sliding along DNA (12–15). The thermal fluctuations of the DNA only contribute as additional offsets to the MSD curves, since the exposure time (20 ms) is much larger than the correlation time of the transverse and longitudinal fluctuations, in the ms range (Supplementary Data). We used the time dependence of the longitudinal MSD and the value of the transverse

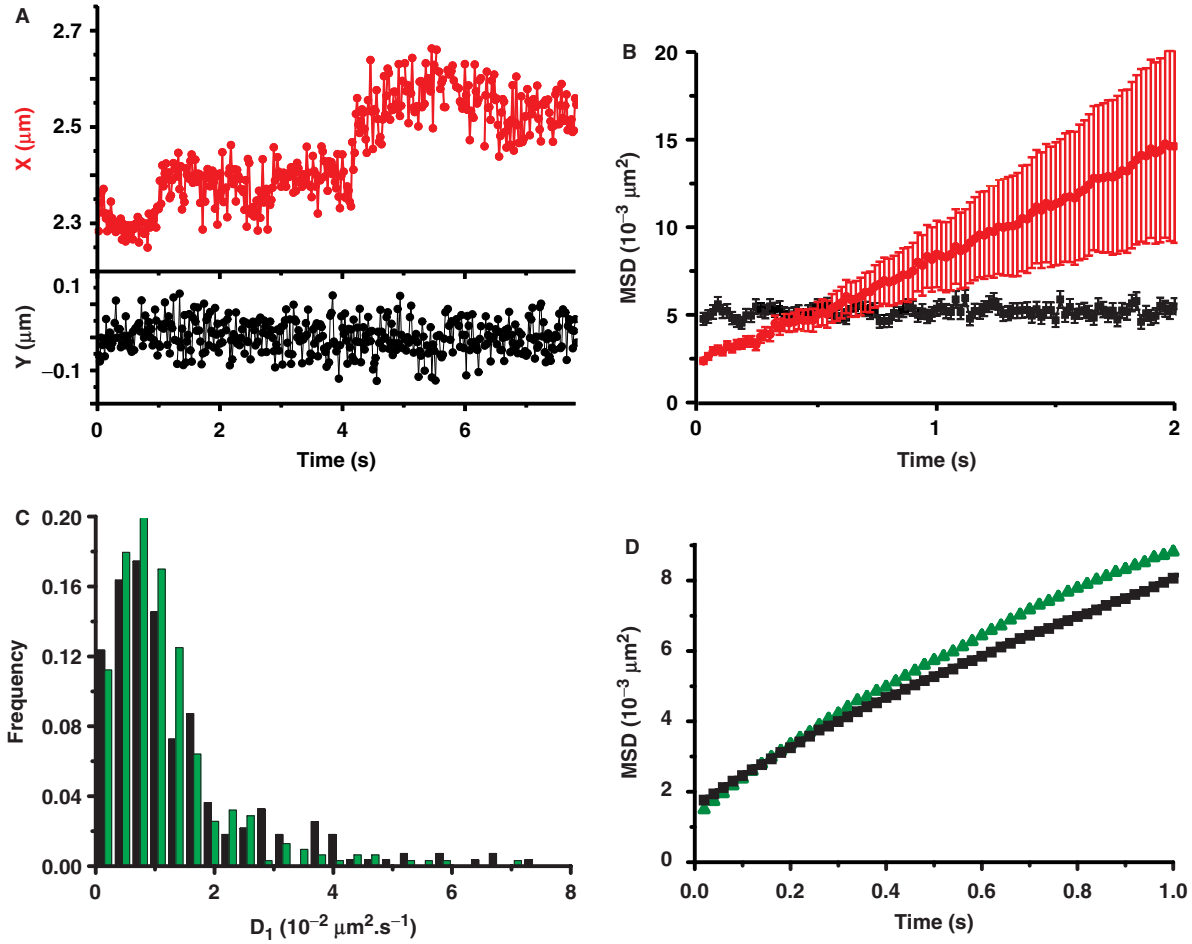

Figure 2. 1D diffusion of EcoRV along elongated DNA. (**A**) Trajectory of a single enzyme interacting with an elongated DNA molecule, aligned along the X direction. The largest variations of the enzyme position are seen along the DNA, for the linear diffusion in this direction superimposes with the DNA thermal fluctuations. The trajectory was recorded in PIPES buffer. (**B**) Mean Square Displacement (MSD) derived from the previous trajectory. The longitudinal MSD (red) depends linearly on time, displaying the sliding of the enzyme along the DNA. The linear diffusion constant D_1 is deduced from the slope of the curve ($2D_1 = 10^{-2}\,\mu m^2/s$). In contrast, the transverse MSD (black) is constant, since the transverse motion of the enzyme is confined. (**C**) Distributions of linear diffusion coefficients in PIPES (green, 266 events) and Tris (black, 379 events). The values were deduced from the MSD of individual trajectories longer than 600 ms (30 frames). (**D**) MSD averaged over individual trajectories in PIPES (green) and in Tris (black).

MSD (generally larger than $2 \times 10^{-3}\,\mu m^2$) to discriminate enzymes interacting with the DNA from the enzymes sticking occasionally to the surface near the DNA, since in the last case both the longitudinal and transverse MSD are constant and below $10^{-3}\,\mu m^2$ (Supplementary Data). For each interaction event, the diffusion constant D_l was derived from the slope of the linearly fitted longitudinal MSD curve after correction for the DNA stretch rate (see Supplementary Data for the detail of the derivation of D_l). The histograms of D_l deduced from single-molecule trajectories in PIPES and Tris are displayed in Figure 2C. For each buffer, we calculated the MSD averaged over all the analysed events (Figure 2D and Supplementary Data for the detail of the calculation). We obtained $D_l = 1.1 \pm 0.2 \times 10^{-2}\,\mu m^2/s$ in PIPES (266 events) and $0.9 \pm 0.2 \times 10^{-2}\,\mu m^2/s$ in Tris (379 events). Similar diffusion constants were found in PB ($0.9 \pm 0.2 \times 10^{-2}\,\mu m^2/s$, 740 events) and HEPES ($1.2 \pm 0.3 \times 10^{-2}\,\mu m^2/s$, 162 events) (data not shown). These results show that the diffusion constant D_l depends only weakly on the buffer.

Jumps of EcoRV along DNA

Some enzyme trajectories along the DNA exhibited large steps (up to 1.8 μm) within two consecutive frames (40 ms)

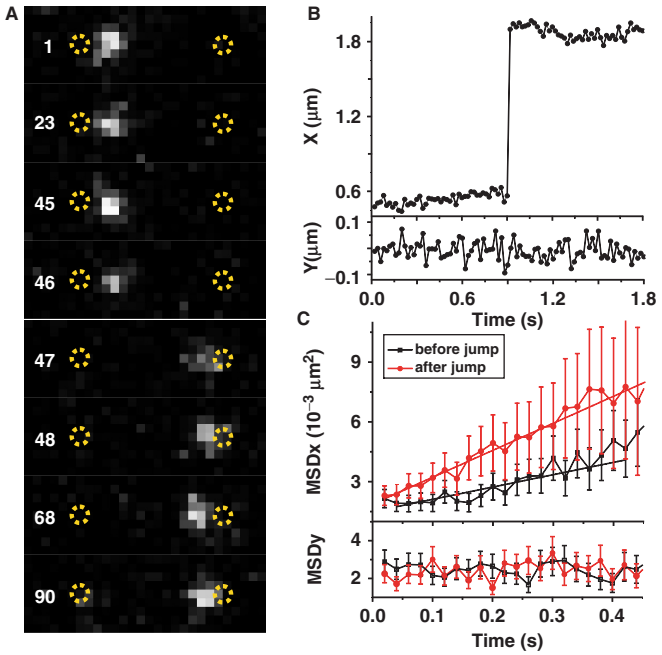

Figure 3. Jump of a single EcoRV along elongated DNA. (**A**) During the interaction of EcoRV with elongated DNA, a large and fast translocation occurs between frames 46 and 47 (numbers indicate the location of the frames in the video sequence, dotted circles indicate the DNA ends). (**B**) A jump of about 1300 nm is detected in the X-trajectory of the enzyme. The length of the jump is much larger than the mean translocation associated with sliding within one frame (20 nm within 20 ms). (**C**) The longitudinal MSD calculated before (0–0.9 s) and after (0.9–1.8 s) the jump display 1D diffusion similar to that observed during events without large jumps. Values of the diffusion constant are 0.34×10^{-2} and $0.54 \times 10^{-2}\,\mu m^2/s$, respectively. The large amplitude of the transverse MSD confirms that the enzyme was interacting with the DNA before and after the jump.

(Figure 3A and B, and Supplementary Data 2, 6 and 7). Large steps were observed with equal probability in both directions. We focussed on steps larger than 200 nm, which are easy to detect since their lengths are larger than both the optical resolution of the microscope and the amplitude of longitudinal fluctuations in the enzyme trajectories before and after the step. The frequency of such large steps, i.e. the number of large steps per interaction event, ranged from 6% in HEPES to 16% in Tris. This frequency is difficult to explain considering a sliding motion with $D_l \sim 10^{-2}\,\mu m^2/s$. Indeed, the mean length $\langle l \rangle$ covered within $\Delta T = 40$ ms in a 1D Brownian motion is $\langle l \rangle = \sqrt{2 D_l \Delta T} \approx 30$ nm, and a statistical analysis of the distribution of the lengths l reveals that, regarding this value of $\langle l \rangle$, the probability of observing steps larger than 200 nm is extremely small (Supplementary Data). Therefore, these steps, which from now on will be called 'large jumps', were attributed to a translocation mechanism which differs from sliding. Large jumps cannot stem from a second enzyme associating immediately after dissociation of the first because, considering the association frequency of EcoRV with the DNA under our experimental conditions (5–10 per min), we estimated the probability of such an event to be smaller than 1% (Supplementary Data). Likewise, large jumps are unlikely to be due to transfers from the DNA to the surface or *vice versa*, since we could discriminate, via the MSD curves, enzymes interacting with the DNA from those stuck to the surface.

The lengths of the large jumps in different buffers are displayed in Figure 4A using normalized complementary cumulative distributions, which give the probability of observing jumps of length s or larger as a function of s during an interaction event. We chose to use complementary cumulative distributions because we focussed on large jumps and such distributions do not depend on the distribution of possible smaller jumps. In contrast to our results regarding the diffusion constant D_l, the occurrence of large jumps as well as the jump length distributions show a noticeable dependence on the buffer (Figure 4A). For PIPES, we found 26 jumps in 266 events (10%) compared to 59 jumps in 379 events for Tris (16%). The jump length distribution follows a similar trend with more than 50% of the large jumps spanning more than 500 nm in Tris, while only less than one third beyond this length are found in PIPES. The influence of the buffer on jump occurrence and distribution are further illustrated by the results obtained in HEPES (10 jumps in 162 events, i.e. 6%) and PB (109 in 740 events, i.e. 15%). Note that, in order to prevent alteration of the estimation of D_l by the large jumps, the events that contained such a translocation were split into two trajectories (before and after the large jump), which were treated as independent events for the determination of D_l.

Experiments under flow

The observation of large jumps in our experiments denotes the existence of a fast translocation mechanism of the enzyme which differs from sliding. A probable mechanism involves dissociation of the enzyme from the DNA followed by re-association after a 3D diffusion. Since the

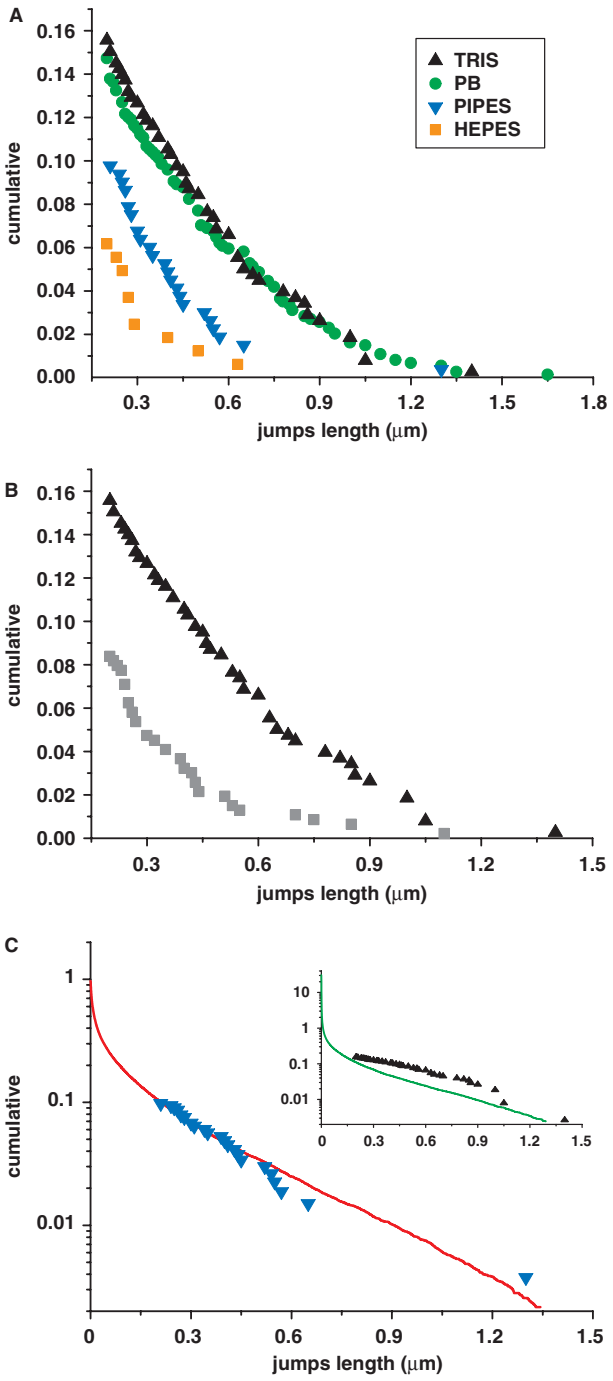

Figure 4. Complementary cumulative distributions of the jump lengths. (**A**) Cumulative jump length distributions in different buffers: Tris (black), PB (green), PIPES (blue) and HEPES (orange). From Tris to HEPES, the probability of observing a large jump (i.e. larger than 200 nm) within an interaction event decreases significantly. The distributions were normalized by dividing the number of observed jumps in interaction events longer than 600 ms (30 frames) by the number of these events. (**B**) The jump distribution in Tris buffer (black) is strongly affected by a flow applied perpendicular to the elongated DNA. The relative number of jumps drops from 0.16 to 0.08 and, under flow, the jump length distribution is shifted to smaller jumps (grey). (**C**) Cumulative jump length distribution provided by numerical simulations with $P = 0.02$ (red) fit the experimental jump length distribution in PIPES (blue), and predict about 1 jump per interaction event. Inset shows the number of large jumps in Tris (black), which remains higher than predicted by the simulations, even with $P = 1$ (green).

3D diffusion coefficient D_3 for EcoRV is about 50 $\mu m^2/s$ (see below), the distance covered by 3D motion within 40 ms can be in the μm range, and thus 3D diffusion may account for the values observed for the length of the large jumps. In principle, another mechanism could involve a fast 1D diffusion in which the enzyme stays bound to the DNA during a fast translocation. To discriminate between 1D and 3D mechanism, we modified the experimental set-up to apply a flow of enzyme solution perpendicular to the elongated DNA. The 3D movement of the enzyme and thus the jump lengths are likely to be affected by the drag of the flow, while it is not expected to influence a fast 1D diffusion during which EcoRV remains firmly bound to the DNA. Flow experiments were carried out in Tris, in which we previously observed the most frequent and largest jumps. When a flow of velocity $v = 70\,\mu m/s$ was applied (see Supplementary Data for an estimation of the flow velocity), the number of jumps per event was reduced to about one half, i.e. jumps larger than 200 nm were observed in only 8% of the interaction events (39 jumps per 470 events) compared to 16% without flow (59 jumps in 379 events). In addition, the jump distribution was significantly shifted to smaller jump lengths, such that only 10% of the recorded jumps were longer than 700 nm compared to 30% in the experiments without flow (Figure 4B). The shift towards smaller jump lengths can be qualitatively accounted for by a simple 3D diffusion model that estimates the length of the jumps affected by the flow. For this purpose, we calculated the distance l_D covered by 3D diffusion during a time t, $l_D \approx \sqrt{D_3\,t}$, and the drift l_v due to the flow during the same time, $l_v = vt$. The time after which the drift overcomes the diffusion (i.e, $l_v > l_D$) is approximately D_3/v^2. Thus, the distribution of the jump lengths is significantly affected for lengths larger than $D_3/v \approx 700$ nm, as observed experimentally. These results provide strong evidence that the large jumps are due to a 3D translocation of the enzymes.

Effect of increasing salt concentration

Changes in ionic conditions are known to modify the kinetics of DNA–protein interactions. In particular, an increase of the concentration of monovalent ions has been shown to strongly decrease the DNA–protein interaction time, while the rate of association to nonspecific DNA is only moderately affected (44). Salt changes are thus expected to affect the relative roles of sliding and hopping/jumping in facilitated diffusion (2,45) (Supplementary Data).

In order to address the effect of ionic conditions on EcoRV sliding and jumping, we performed experiments at NaCl concentrations ranging from 10 mM to 60 mM, the latter [NaCl] providing an ionic strength (~110 mM) comparable to physiological conditions. Salt-dependent experiments were carried out in PIPES. For each [NaCl], we recorded hundreds of interaction events, from which we derived the mean DNA–EcoRV interaction time (see Supplementary Data for details). As expected, the interaction time was strongly reduced with increasing [NaCl] (Figure 5C), ranging from 4.4 ± 1 s at 10 mM NaCl to 0.3 ± 0.1 s at 60 mM NaCl.

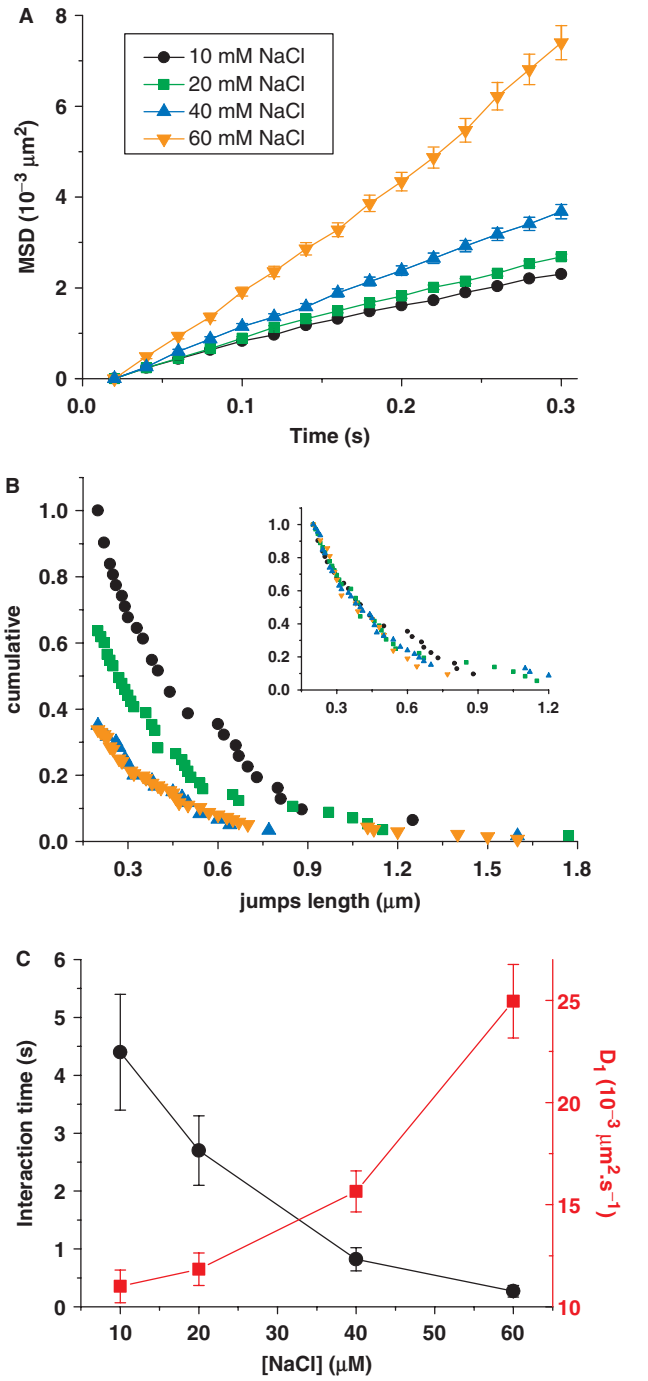

Figure 5. Dependence of sliding and jumping on the NaCl concentration. (A) Averaged MSD derived from interaction events recorded at salt concentrations ranging from 10 to 60 mM NaCl. The MSDs at 10 mM (black) and 20 mM (green) NaCl are similar, whereas a significant increase of the MSD slope is observed with increasing salt concentration to 40 mM (blue) and 60 mM (orange). (B) Complementary jump length distributions at different salt concentrations. The distributions were normalized against the distribution at 10 mM NaCl (black). The total number of large jumps decreases with increasing salt concentration (green: 20 mM, blue: 40 mM, orange: 60 mM NaCl), but the shape of the distribution remains identical (inset, all the distributions normalized against the same number of large jumps). (C) DNA–EcoRV interaction time (black) and diffusion constant (red) as a function of [NaCl]. The interaction time is strongly reduced with increasing the salt concentration, whereas a significant increase of the diffusion coefficient is observed only for the highest values of [NaCl].

The diffusion constants of the enzyme at different [NaCl] were derived from the averaged MSD (Figure 5A). At 20 mM NaCl, the diffusion constant was $D_1 = 1.2 \pm 0.1 \times 10^{-2}\,\mu m^2/s$ (217 events), i.e. similar to that obtained at 10 mM NaCl ($D_1 = 1.1 \pm 0.1 \times 10^{-2}\,\mu m^2/s$ (168 events)). For larger [NaCl], we observed a significant increase of the mean diffusion constant, $D_1 = 1.6 \pm 0.1 \times 10^{-2}\,\mu m^2/s$ at 40 mM NaCl (120 events) and $D_1 = 2.5 \pm 0.2 \times 10^{-2}\,\mu m^2/s$ at 60 mM NaCl (179 events) (Figure 5A and C). For each [NaCl], we also determined the complementary cumulative length distribution of the large jumps, i.e. larger than 200 nm. The number of large jumps during DNA–EcoRV interaction was found to decrease monotonously with increasing salt concentration (Figure 5B): at 60 mM NaCl, the number of large jumps was smaller by a factor 2.5 compared to 10 mM NaCl. The shape of the distribution, however, did not depend on the salt concentration (inset in Figure 5B).

DISCUSSION

Linear diffusion coefficient

We derived from our experiments at low [NaCl] (i.e. in conditions where D_1 is not affected by small jumps, see below) a linear diffusion constant D_1 of approximately $10^{-2}\,\mu m^2/s$, similar to that reported in recent single-molecule experiments reporting the diffusion of other proteins along DNA (12–16). D_1 is three orders of magnitude smaller than the 3D diffusion coefficient D_3, which is about $50\,\mu m^2/s$ for EcoRV (see below). This drastic reduction is usually attributed to two factors: the hydrodynamics of the enzyme sliding along DNA and the modulation of the DNA–protein interaction potential during the 1D walk. If one models the enzyme by a sphere of radius r that diffuses linearly along the DNA helix, the diffusion constant can be written as $D_1^{hydro} = 3h^2D_3/16\pi^2r^2$, where $h = 3.4$ nm is the pitch of the DNA helix (46). Using Fluorescence Correlation Spectroscopy, we measured the hydrodynamic radius $r = 4.0 \pm 0.1$ nm of EcoRV-Cy3B in PIPES (Supplementary Data). This value yields $D_3 = k_BT/6\pi\eta r = 54\,\mu m^2/s$ at $T = 300$ K in water ($\eta = 10^{-3}$ Pa.s) and $D_1^{hydro} = 0.74\,\mu m^2/s$. Additional reduction of the linear diffusion constant can be attributed to a modulation of the DNA–protein interaction during linear diffusion. Considering a sequence-dependent energy landscape of roughness σ, the diffusion constant D_1 reads (21): $D_1 = D_1^{hydro}\,(1 + \beta^2\sigma^2/2)^{1/2}\,\exp(-7\beta^2\sigma^2/4)$, with $\beta = 1/k_BT$. Using $D_1 = 10^{-2}\,\mu m^2/s$, we found $\sigma = 1.6\,k_BT$. This value is below $2k_BT$, which has been predicted to be the upper limit for accelerated target location involving 1D motion (21). The relatively large value of σ and the subsequent slow diffusion could be rationalized by the large contact region between EcoRV and the DNA, spanning at least 10 bp (32). The diffusion constant we measured is somewhat below that derived from kinetic experiments with EcoRV, ranging from $3 \times 10^{-2}\,\mu m^2/s$ to $10^{-1}\,\mu m^2/s$ (30,47). These studies, however, only considered sliding in the model used for fitting the kinetic data,

and were carried out at higher ionic strength. Hence these values are difficult to compare to those obtained from our direct observation of 1D motion along DNA at low salt concentration.

Numerical simulations

In order to account for the observed jump frequency and length distributions, we performed numerical Monte-Carlo simulations based on a combination of sliding (1D diffusion along the DNA) and jumping (3D diffusion) (details are given in Supplementary Data). We focussed on experimental data obtained at 10 mM [NaCl] for comparison with numerical results. Accordingly, we simulated the trajectory of an enzyme able to slide along a static, straight DNA molecule of finite length with a diffusion constant $D_1 = 10^{-2}\,\mu m^2/s$. During its sliding motion, the enzyme could dissociate from the DNA. After dissociation, we simulated its 3D trajectory until a potential encounter with the DNA molecule. Upon the encounter, the protein re-associates to the DNA with a finite probability P, i.e. after each encounter, the enzyme could resume its 3D diffusion with a probability $1 - P$. The surface onto which the DNA was attached was included in the simulations: during 3D diffusion, the enzyme could be reflected by an infinite plane located 70 nm below the DNA, this distance corresponding to the mean amplitude of the thermal transverse DNA fluctuations. A simulation was stopped when no encounter between the DNA and the enzyme occurred after a 3D walk of 40 ms. The photobleaching of the dye was also taken into account in the simulations (Supplementary Data). Ten thousand interaction events were simulated with enzyme starting points uniformly distributed along the DNA. Only simulated trajectories longer than 0.6 s were considered for generating jump length cumulative distributions in order to be consistent with our experimental results. The only adjustable parameter in our simulations is the probability P of binding to the DNA upon encounter. With decreasing P, the number of large jumps decreases monotonously, and the jump length distribution derived from the numerical simulations with $P = 0.02$ is in excellent agreement with the experimental PIPES data (Figure 4C). For the other buffers the agreement is only qualitative, and, for instance, the number of large jumps observed in Tris remains slightly larger than predicted by the simulations, even with $P = 1$ (Figure 4C). Regarding the simplicity of our model, which does not include, for instance, the DNA fluctuations or the electrostatic interactions between the protein and the DNA, the fact that the probability of observing large jumps derived from our experiments can be qualitatively accounted for by our simulations is a further support for the conclusion that large jumps reported here stem from 3D translocations on the DNA.

Interplay of 1D and 3D diffusion

We have considered so far only large jumps, i.e. translocations larger than 200 nm. However, 3D excursions between two DNA sites separated by less than 200 nm are likely to occur. These small jumps are difficult to distinguish from sliding by optical means. According to the simulations, about one small jump occurred per interaction event in PIPES (Figure 4C). Moreover, the significantly higher number of large jumps observed in Tris together with the simulation results for $P = 1$ suggest that the number of invisible small jumps per interaction event might be up to a few tens per interaction event, depending on the experimental conditions. Although these values are rough estimations regarding the simplicity of the model, they are in qualitative agreement with previous theoretical works which predicted that small jumps occur more frequently than large-scale jumps (4,26,48).

The existence of small jumps might affect the estimation of the diffusion constant D_1, since what we have considered so far as a sliding motion (i.e. an interaction event without large jumps) reflects in fact the combination of sliding phases and small jumps. These small invisible jumps can lead to an 'apparent' 1D diffusion constant larger than that expected from pure sliding, because enzyme motion along DNA may be much faster when performed by a 3D than by a 1D mechanism. The effect of small jumps on the apparent diffusion constant, however, is significant only if the distance covered by sliding is comparable or smaller than that covered by 3D translocations during an interaction event. With increasing [NaCl], we observed a strong reduction (15-fold) of the interaction time while the jump distribution was almost maintained. Therefore, the duration of the sliding phases was strongly reduced, whereas the number of small jumps was not significantly altered. As a consequence, the distance covered by sliding was strongly reduced, whereas that covered by jumping remained almost unchanged, resulting in an increase of the apparent diffusion constant. Importantly, the diffusion coefficient does not change significantly for [NaCl] between 10 and 20 mM (Figure 5C), which confirms that our measurement of D_1 performed at low [NaCl] is not affected by small jumps.

A significant number of small jumps per interaction event can reconcile ensemble measurements that provided very different estimations for the sliding length, i.e. the DNA length explored by the enzyme during a sliding phase. This length was inferred to be larger than 1000 bp in studies where the length of non-specific DNA flanking an EcoRV recognition site was varied (30), whereas it was found to be below 100 bp in experiments involving DNA with two recognition sites in close proximity (34). This discrepancy could be explained by considering that, due to hopping/jumping, the DNA length effectively explored by the protein after an initial binding to the nucleic acid could be much larger than the sliding length itself. Finally, we point out that the observed jump distributions were measured on an elongated substrate, whereas free DNA in solution adopts a coiled conformation. For small jumps, elongated and coiled conformations should be comparable as the DNA is expected to be rigid for lengths smaller than the DNA persistence length (50 nm). The coiled conformation, however, considerably favours large jumps, which can not only occur onto DNA sequences nearby, but also to distant sequences which nevertheless are close in space (24). Therefore, it is likely that the average number of jumps per interaction

event is significantly larger for coiled DNA than for elongated DNA (38).

In summary, we report here the first direct observation of sliding and jumping for individual EcoRV enzymes interacting with nonspecific DNA. Our investigation regarding both 1D Brownian motion (sliding) and 3D translocations (jumping), combined with numerical simulations and salt-dependent experiments, allowed us to quantitatively estimate the respective part of these two processes in the facilitated diffusion of EcoRV under our experimental conditions. As far as we know, a jumping process has never been directly observed earlier with any DNA-binding protein, although it was postulated in many previously published experimental and theoretical studies. The contribution of hopping/jumping to facilitated diffusion, however, might differ from protein to protein, depending on both the structure and the biological function of the protein.

The small jumps that are inferred from our study can answer the problem of target search within a crowded environment (20) as they enable the enzyme to bypass obstacles of typical protein size that could block sliding. On the other hand, large jumps favour the exploration of distant DNA sites, especially when the DNA is in a coiled conformation, thus accelerating target site location compared to sliding alone.

SUPPLEMENTARY DATA

Supplementary Data are available at NAR Online.

ACKNOWLEDGEMENTS

This work was supported by funds from Centre National de la Recherche Scientifique, Institut National de la Santé et de la Recherche Médicale, Egide, Ministère de la Recherche (ACI Nanosciences NR069), Deutscher Akademischer Austausch Dienst, Deutschen Forschungsgemeinschaft and European Union. A.B. was supported by the Fondation pour la Recherche Médicale (Accueil Chercheur Etranger 20051206325). We thank Pierre Neveu and Jean-François Allemand for FCS measurements, and Maxime Dahan for discussions and support. Funding to pay the Open Access publication charges for this article was provided by Ministère de la Recherche (ACI Nanosciences NR069).

Conflict of interest statement. None declared.

REFERENCES

1. Riggs,A.D., Bourgeois,S. and Cohn,M. (1970) The lac repressor-operator interaction. 3. Kinetic studies. *J. Mol. Biol.*, **53**, 401–417.
2. Berg,O.G., Winter,R.B. and von Hippel,P.H. (1981) Diffusion-driven mechanisms of protein translocation on nucleic acids. 1. Models and theory. *Biochemistry*, **20**, 6929–6948.
3. Winter,R.B., Berg,O.G. and von Hippel,P.H. (1981) Diffusion-driven mechanisms of protein translocation on nucleic acids. 3. The Escherichia coli lac repressor—operator interaction: kinetic measurements and conclusions. *Biochemistry*, **20**, 6961–6977.
4. von Hippel,P. and Berg,O. (1989) Facilitated target location in biological systems. *J. Biol. Chem.*, **264**, 675–678.
5. Halford,S.E. (2001) Hopping, jumping and looping by restriction enzymes. *Biochem. Soc. Trans.*, **29**, 363–373.
6. Halford,S.E. and Marko,J.F. (2004) How do site-specific DNA-binding proteins find their targets? *Nucleic Acids Res.*, **32**, 3040–3052.
7. Widom,J. (2005) Target site localization by site-specific, DNA-binding proteins. *Proc. Natl Acad. Sci. USA*, **102**, 16909–16910.
8. Shimamoto,N. (1999) One-dimensional diffusion of proteins along DNA. Its biological and chemical significance revealed by single-molecule measurements. *J. Biol. Chem.*, **274**, 15293–15296.
9. Adam,G. and Delbrück,M. (1968) In Rich,A. and Davidson,N. (eds), *Structural Chemistry and Molecular Biology*. Freeman, San Francisco, pp. 198–215.
10. Richter,P.H. and Eigen,M. (1974) Diffusion controlled reaction rates in spheroidal geometry. Application to repressor—operator association and membrane bound enzymes. *Biophys. Chem.*, **2**, 255–263.
11. Kabata,H., Kurosawa,O., Arai,I., Washizu,M., Margarson,S.A., Glass,R.E. and Shimamoto,N. (1993) Visualization of single molecules of RNA polymerase sliding along DNA. *Science*, **262**, 1561–1563.
12. Granéli,A., Yeykal,C.C., Robertson,R.B. and Greene,E.C. (2006) Long-distance lateral diffusion of human Rad51 on double-stranded DNA. *Proc. Natl Acad. Sci. USA*, **103**, 1221–1226.
13. Blainey,P.C., van Oijen,A.M., Banerjee,A., Verdine,G.L. and Xie,X.S. (2006) A base-excision DNA-repair protein finds intrahelical lesion bases by fast sliding in contact with DNA. *Proc. Natl Acad. Sci. USA*, **103**, 5752–5757.
14. Wang,Y.M., Austin,R.H. and Cox,E.C. (2006) Single molecule measurements of repressor protein 1D diffusion on DNA. *Phys. Rev. Lett.*, **97**, 048302.
15. Kim,J.H. and Larson,R.G. (2007) Single-molecule analysis of 1D diffusion and transcription elongation of T7 RNA polymerase along individual stretched DNA molecules. *Nucleic Acids Res.*, **35**, 3848–3858.
16. Gorman,J., Chowdhury,A., Surtees,J.A., Shimada,J., Reichman,D.R., Alani,E. and Greene,E.C. (2007) Dynamic basis for one-dimensional DNA scanning by the mismatch repair complex Msh2-Msh6. *Mol. Cell*, **28**, 359–370.
17. Elf,J., Li,G.W. and Xie,X.S. (2007) Probing transcription factor dynamics at the single-molecule level in a living cell. *Science*, **316**, 1191–1194.
18. Gowers,D.M., Wilson,G.G. and Halford,S.E. (2005) Measurement of the contributions of 1D and 3D pathways to the translocation of a protein along DNA. *Proc. Natl Acad. Sci. USA*, **102**, 15883–15888.
19. Gerland,U., Moroz,J.D. and Hwa,T. (2002) Physical constraints and functional characteristics of transcription factor-DNA interaction. *Proc. Natl Acad. Sci. USA*, **99**, 12015–12020.
20. Flyvbjerg,H., Keatch,S.A. and Dryden,D.T.F. (2006) Strong physical constraints on sequence-specific target location by proteins on DNA molecules. *Nucleic Acids Res.*, **34**, 2550–2557.
21. Slutsky,M. and Mirny,L.A. (2004) Kinetics of protein-DNA interaction: facilitated target location in sequence-dependent potential. *Biophys. J.*, **87**, 4021–4035.
22. Coppey,M., Bénichou,O., Voituriez,R. and Moreau,M. (2004) Kinetics of target site localization of a protein on DNA: A stochastic approach. *Biophys. J.*, **87**, 1640–1649.
23. Lomholt,M.A., Ambjornsson,T. and Metzler,R. (2005) Optimal target search on a fast-folding polymer chain with volume exchange. *Phys. Rev. Lett.*, **95**, 260603.
24. Hu,T., Grosberg,A.Y. and Shklovskii,B.I. (2006) How proteins search for their specific sites on DNA: The role of DNA conformation. *Biophys. J.*, **90**, 2731–2744.
25. Klenin,K.V., Merlitz,H., Langowski,J. and Wu,C.X. (2006) Facilitated diffusion of DNA-binding proteins. *Phys. Rev. Lett.*, **96**, 018104.
26. Kolesov,G., Wunderlich,Z., Laikova,O.N., Gelfand,M.S. and Mirny,L.A. (2007) How gene order is influenced by the biophysics of transcription regulation. *Proc. Natl Acad. Sci. USA*, **104**, 13948–13953.

27. Ehbrecht,H.J., Pingoud,A., Urbanke,C., Maass,G. and Gualerzi,C. (1985) Linear diffusion of restriction endonucleases on DNA. *J. Biol. Chem.*, **260**, 6160–6166.
28. Pingoud,A. and Jeltsch,A. (2001) Structure and function of type II restriction endonucleases. *Nucleic Acids Res.*, **29**, 3705–3727.
29. Taylor,J.D., Badcoe,I.G., Clarke,A.R. and Halford,S.E. (1991) EcoRV restriction endonuclease binds all DNA sequences with equal affinity. *Biochemistry*, **30**, 8743–8753.
30. Jeltsch,A. and Pingoud,A. (1998) Kinetic characterization of linear diffusion of the restriction endonuclease EcoRV on DNA. *Biochemistry*, **37**, 2160–2169.
31. Jeltsch,A., Wenz,C., Stahl,F. and Pingoud,A. (1996) Linear diffusion of the restriction endonuclease EcoRV on DNA is essential for the in vivo function of the enzyme. *EMBO J.*, **15**, 5104–5111.
32. Winkler,F.K., Banner,D.W., Oefner,C., Tsernoglou,D., Brown,R.S., Heathman,S.P., Bryan,R.K., Martin,P.D., Petratos,K. and Wilson,K.S. (1993) The crystal-structure of ecorv endonuclease and of its complexes with cognate and Non-cognate DNA fragments. *EMBO J.*, **12**, 1781–1795.
33. Schulze,C., Jeltsch,A., Franke,I., Urbanke,C. and Pingoud,A. (1998) Crosslinking the EcoRV restriction endonuclease across the DNA-binding site reveals transient intermediates and conformational changes of the enzyme during DNA binding and catalytic turnover. *EMBO J.*, **17**, 6757–6766.
34. Stanford,N.P., Szczelkun,M.D., Marko,J.F. and Halford,S.E. (2000) One- and three-dimensional pathways for proteins to reach specific DNA sites. *EMBO J.*, **19**, 6546–6557.
35. Jeltsch,A. and Urbanke,C. (2004) In Pingoud,A. (ed.), *Nucleic Acids and Molecular Biology*. Springer-Verlag, Berlin, Vol. 14, pp. 95–110.
36. Gowers,D.M. and Halford,S.E. (2003) Protein motion from non-specific to specific DNA by three-dimensional routes aided by supercoiling. *EMBO J.*, **22**, 1410–1418.
37. Seidel,R., van Noort,J., van der Scheer,C., Bloom,J.G., Dekker,N.H., Dutta,C.F., Blundell,A., Robinson,T., Firman,K. and Dekker,C. (2004) Real-time observation of DNA translocation by the type I restriction modification enzyme EcoR124I. *Nat. Struct. Mol. Biol.*, **11**, 838–843.
38. van den Broek,B., Noom,M.C. and Wuite,G.J. (2005) DNA-tension dependence of restriction enzyme activity reveals mechanochemical properties of the reaction pathway. *Nucleic Acids Res.*, **33**, 2676–2684.
39. Gemmen,G.J., Millin,R. and Smith,D.E. (2006) DNA looping by two-site restriction endonucleases: heterogeneous probability distributions for loop size and unbinding force. *Nucleic Acids Res.*, **34**, 2864–2877.
40. Crut,A., Géron-Landre,B., Bonnet,I., Bonneau,S., Desbiolles,P. and Escudé,C. (2005) Detection of single DNA molecules by multicolor quantum-dot end-labeling. *Nucleic Acids Res.*, **33**, e98.
41. Crut,A., Lasne,D., Allemand,J.F., Dahan,M. and Desbiolles,P. (2003) Transverse fluctuations of single DNA molecules attached at both extremities to a surface. *Phys. Rev. E*, **67**, 051910.
42. Granéli,A., Yeykal,C.C., Prasad,T.K. and Greene,E.C. (2006) Organized arrays of individual DNA molecules tethered to supported lipid bilayers. *Langmuir*, **22**, 292–299.
43. Wenner,J.R. and Bloomfield,V.A. (1999) Buffer effects on EcoRV kinetics as measured by fluorescent staining and digital imaging of plasmid cleavage. *Anal. Biochem.*, **268**, 201–212.
44. Lohman,T.M. (1986) Kinetics of protein-nucleic acid interactions: use of salt effects to probe mechanisms of interaction. *CRC Crit. Rev. Biochem.*, **19**, 191–245.
45. Halford,S.E. and Szczelkun,M.D. (2002) How to get from A to B: strategies for analysing protein motion on DNA. *Eur. Biophys. J.*, **31**, 257–267.
46. Schurr,J.M. (1975) The one-dimensional diffusion coefficient of proteins absorbed on DNA hydrodynamic considerations. *Biophys. Chem.*, **9**, 413–414.
47. Erskine,S.G., Baldwin,G.S. and Halford,S.E. (1997) Rapid-reaction analysis of plasmid DNA cleavage by the EcoRV restriction endonuclease. *Biochemistry*, **36**, 7567–7576.
48. Berg,O.G. (1978) On diffusion-controlled dissociation. *Chem. Phys.*, **31**, 47–57.